Cybershake NZ v17.9: New Zealand simulation-based probabilistic seismic hazard analysis

K. Tarbali[1], B.A. Bradley[1], J. Huang[1], V. Polak[2], D. Lagrava[1], J. Motha[1] & S. Sung[2]

[1] Department of Civil and Natural Resources Engineering, University of Canterbury, Christchurch, New Zealand.
[2] QuakeCoRE, University of Canterbury, Christchurch, New Zealand.

ABSTRACT

This paper presents the computational workflow and preliminary results of probabilistic seismic hazard analysis (PSHA) in New Zealand based on physics-based ground motion simulations ('Cybershake NZ'). In the current work completed to date, the Graves and Pitarka (2010, 2015) hybrid broadband ground motion simulation approach is utilized considering a transition frequency of 0.25 Hz, a detailed crustal model with a grid spacing of 0.4 km, and an empirically-calibrated local site response model. Variation in hypocentre location and slip distribution are considered to partially account for the variability in ground motion characteristics. Ruptures from the distributed seismicity model are considered in the total hazard via empirical ground motion models. Intensity measures for sample scenario ruptures and subsequently generated hazard curves are presented here. Treatment of uncertainty in the context of simulation-based PSHA is discussed. Lastly, improvements for future versions of the ongoing effort are outlined.

1 INTRODUCTION

Probabilistic seismic hazard analysis (PSHA) is a key component in seismic design and performance assessment of engineered systems, which considers the likelihood of possible earthquake scenarios in the region of interest using an earthquake rupture forecast (ERF) and combines it with the estimates of exceedance rate for given ground motion levels using a ground motion model (GMM). Accurate representations of rupture characteristics, wave propagation, and subsurface soil behaviour are necessary for PSHA. Conventionally, simplified models are used to represent rupture characteristics (mostly using rupture magnitude) and resulting ground motions (utilizing empirical GMMs), which neglects the inherent physical complexities in earthquake rupture and ground motion properties, such as slip heterogeneity, rupture directivity, and basin depth and edge effects, among others. In addition, issues such as the paucity of ground

motions recorded from large magnitude ruptures in the near-fault region, assumptions regarding the ergodicity in ground motion properties for a given site and rupture characteristics, and the large aleatory variability and epistemic uncertainty in empirical GMMs (Bommer et al. 2010, Bommer et al. 2005, Strasser et al. 2009) persuade utilizing alternative approaches for seismic hazard analysis. The simulation methodologies strive to consider phenomena such as slip heterogeneity, stress drop, hypocenter location, rupture velocity, detailed characterization of the Earth's crust, basin generated waves, nonlinear site effects, etc. Validation of simulated ground motions against the observed ground motions in the past events (Bradley et al. 2017b, Goulet et al. 2015, Graves and Pitarka 2010, 2015, Taborda et al. 2016, Taborda and Bielak 2013) demonstrates the capabilities of simulations to be used for seismic hazard analyses, such as through the 'Cybershake' project in Southern California (Graves et al. 2011).

This paper presents the computational workflow and preliminary results of the first stable version (v17.9) of utilizing physics-based ground motion simulation approach for seismic hazard analysis in New Zealand (Cybershake NZ v17.9). In the next section, the computational workflow is presented and its different components are discussed. Subsequently, illustrative outputs of the conducted analyses are shown and further discussions regarding improvements for future versions of this ongoing effort are presented.

2 COMPUTATIONAL WORKFLOW

Cybershake NZ v17.9 considers different approaches for calculating the hazards from finite faults and distributed seismicity sources in Stirling et al. (2012) (as presented in Figure 1). This is due to a large number of distributed seismicity sources across the country and the computational cost of ground motion simulation. Therefore, ground motions from distributed seismicity sources are calculated using empirical GMMs and physics-based simulations are conducted only for the finite fault sources. As the available computational resources increase in the future, distributed seismicity sources can be included in the simulation branch in Figure 1 (for regions where the seismic hazard is dominated by these sources). In the v17.9 execution, ground motions are simulated using the hybrid broadband simulation approach of Graves and Pitarka (2010, 2015) considering a transition frequency of 0.25 Hz, a detailed crustal model with a grid spacing of 0.4 km, a minimum shear wave velocity of 500 m/s, and the empirically-calibrated local site response model of Campbell and Bozorgnia (2014).

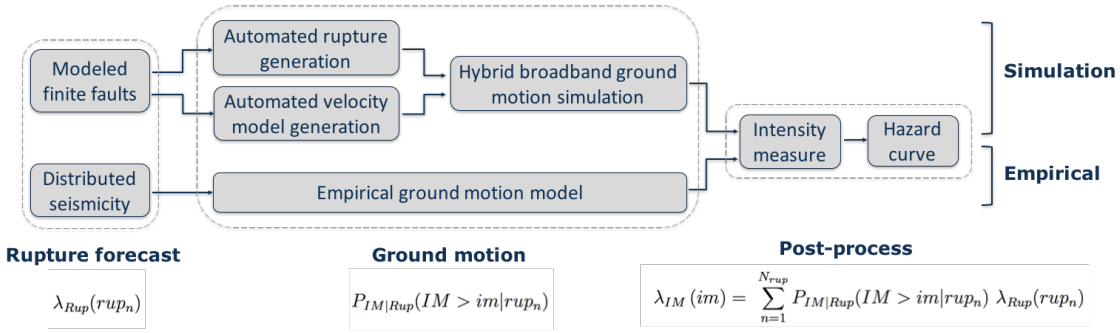

Figure 1. Computational workflow of Cybershake NZ v17.9: PSHA utilizing physics-based ground motion simulation.

The present simulation-based PSHA of California via the SCEC Cybershake effort (Graves et al. 2011) utilizes reciprocity due to the larger number of considered sources (i.e., 10000 – resulting in 415,000 rupture realizations) in comparison to the number of recording stations (250). In contrast, this study uses a forward simulation approach as the total number of finite faults in Stirling et al. (2012) (i.e., 536), and the resulting rupture realizations (i.e., 3222 in the current version as elaborated on subsequently) are significantly less than the number of recording stations (19604 in the current recording stations utilized). Note the much larger number of recording stations (19604 vs. 250), which is based on feedback as to the desired level of spatial resolution for simulation outputs for earthquake engineers. The other difference is that site effects are considered in Cybershake NZ, albeit via a generic empirical model (i.e., Campbell and Bozorgnia (2014)). The desire to directly use forward simulation is also based on implementing a workflow that is future-proof to the inclusion of nonlinearities in ground motion simulation (Roten et al. 2017, Taborda et al. 2012), which we aim to include in 2019.

2.1 Kinematic rupture generation

The ground motion simulation workflow presented in Figure 1 includes automated generation of kinematic ruptures (Graves and Pitarka 2015) based on the corresponding fault geometry, seismic moment, rake angle, and the considered hypocentre location. Figure 2 illustrates all of the shallow crustal faults from Stirling et al. (2012) considered in this study. Note that subduction ruptures were excluded in v17.9 as the ground motion simulation validation efforts (in New Zealand and elsewhere) have mostly focused on shallow crustal events (e.g., Bradley et al. 2017a, Bradley et al. 2017b, Goulet et al. 2015).

Variation in hypocentre location and slip distribution are considered to partially account for the variability in ground motion characteristics. For the intent of v17.9 we consider a coarse representation of these uncertainties. The number of hypocentres along the strike direction is determined based on the length of ruptures, specifically at 20 km intervals. A single hypocentre (at the along-strike midpoint) is considered for ruptures with lengths smaller than 20km. All hypocentres along the strike direction are located at a constant

down-dip depth (i.e., corresponding to 0.6 times the down-dip width of the rupture) (Mai et al. 2005). Three slip realizations are generated for a given hypocentre location using the kinematic rupture generation of Graves and Pitarka (2015).

Excluding small magnitude offshore ruptures with velocity model domains entirely in the ocean (i.e. sources that don't produce any appreciable shaking on land), 410 sources were considered (160 and 250 in the South and North Islands, respectively). Given the above-mentioned scheme for generating hypocentres and slip realizations, 1566 and 1656 distinct ruptures are generated for the corresponding sources in the South and North Islands, respectively. At the current stage of the project, we have simulated ground motions for 50 faults in the South Island, which include 546 simulations.

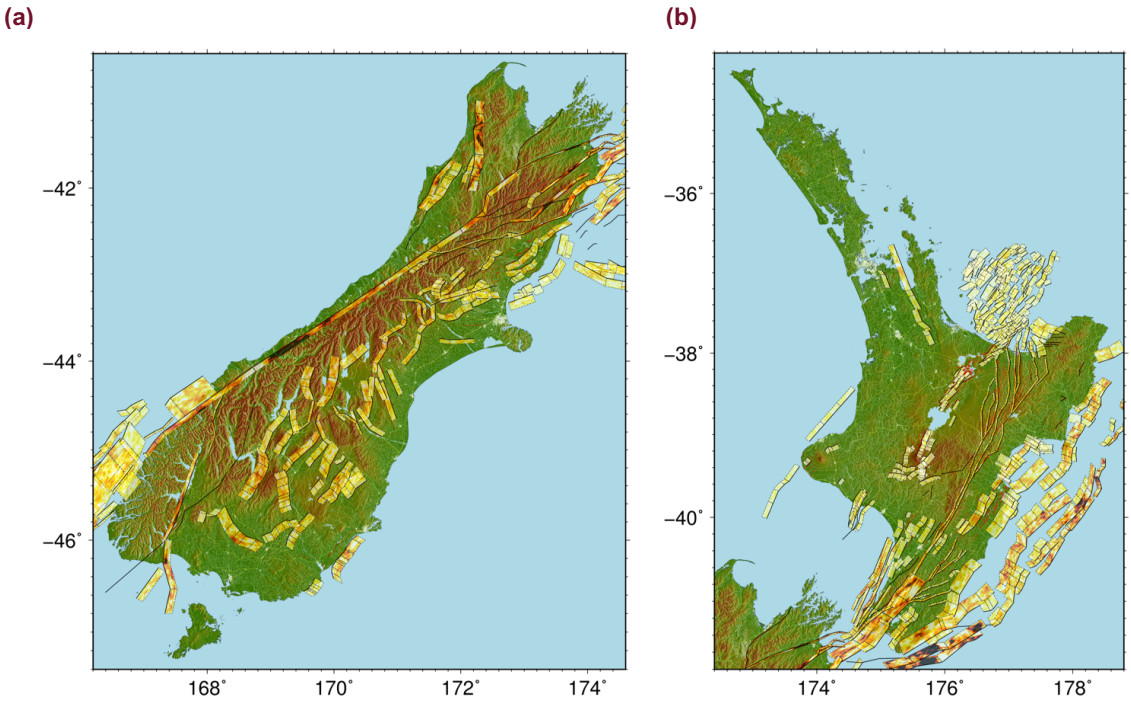

Figure 2. Shallow crustal finite faults in Stirling et al. (2012) considered in Cybershake NZ v17.9: (a) South Island; and (b) North Island.

Rupture moment magnitudes were calculated based on Leonard (2010) relationship, considering a modification to their seismogenic depth from that specified in Stirling et al. (2012) directly. Considering that the lower seismogenic depth of faults are inferred based on the distributed seismicity recordings (Stirling et al. 2012), and past investigations regarding the occurrence of rupture beyond the inferred seismogenic depth (King and Wesnousky 2007), ruptures with lower seismogenic depths of 12 km (or larger) in Stirling et al. (2012) are considered to extend 3km beyond the corresponding lower seismogenic depth. A similar approach was considered by Graves and Pitarka (2015) and is shown to alleviate the inconsistency in the long-period content of simulated ground motions in comparison to observations. Note that Leonard (2010) relationship is also established based on assuming that ruptures beyond the inferred seismogenic depths can occur, and this same approach was adopted by Bradley et al. (2017a) for simulation of Alpine Fault earthquakes in NZ.

2.2 Simulation domain generation

Simulation domains for the considered sources are generated utilizing a detailed velocity model of Lee et al. (2017) for the Canterbury region and Eberhart-Phillips et al. (2010) for the rest of New Zealand. The simulation domain for each and every fault is generated using an optimization algorithm which maximizes the land coverage of the simulation domain (in order to remove the unnecessary computational burden of simulating ground motions offshore). The initial horizontal extents of the domain are calculated by computing a boundary around the fault that corresponds to a peak ground velocity (PGV) of 5 cm/s using the Bradley (2013) empirical GMM. This initial domain is rotated to align in its largest extent with the centre line of the country landmass. Then, if the domain boundaries extend offshore, the extents are reduced considering that the domain edges should be 15 km away from the fault edges and 5km from the shoreline (whichever is the largest). Figure 3 illustrates this process for three faults, illustrating the initial and optimized domains. Note that the criteria utilized for the optimization are iteratively determined considering different rupture sizes and the shape of New Zealand. The depth of simulation velocity models is calculated considering the corresponding rupture magnitude and the minimum depth that enables capturing the downward radiated waves.

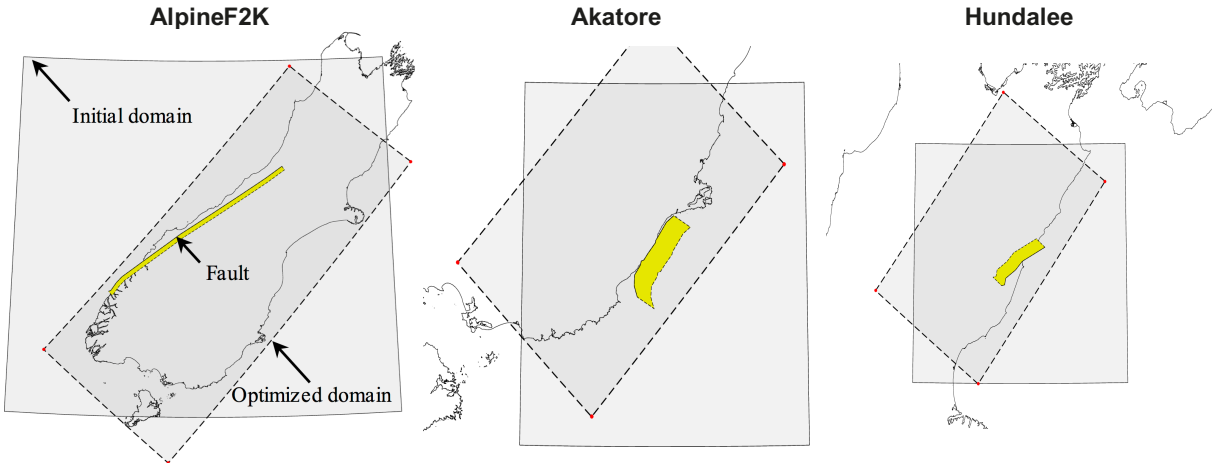

Figure 3. Automated velocity model generation and optimization of the land coverage for three illustrative faults.

2.3 Ground motion recording stations

In order to have a consistent grid of points on the surface to store the simulated ground motions and combine the results to obtain seismic hazard, a nation-wide grid of recording stations is generated (as shown in Figure 4). This grid has a non-uniform spatial density which is a function of population density and sub-surface soil condition. The population data provides an appropriate constraint to have a coarser grid size in mountainous regions, and finer grid sizes in highly populated regions (which provides a robust means for site-specific PSHA). Considering the depth corresponding to the shear wave velocity of 500 m/s, a denser grid is also obtained in regions with deep sedimentary basins. All the strong-motion stations of GeoNet (https://github.com/GeoNet/delta) are included in the generated grid in order to provide a means to compare the simulated ground motions with future ruptures (if the simulation assumptions are close to the rupture characteristics).

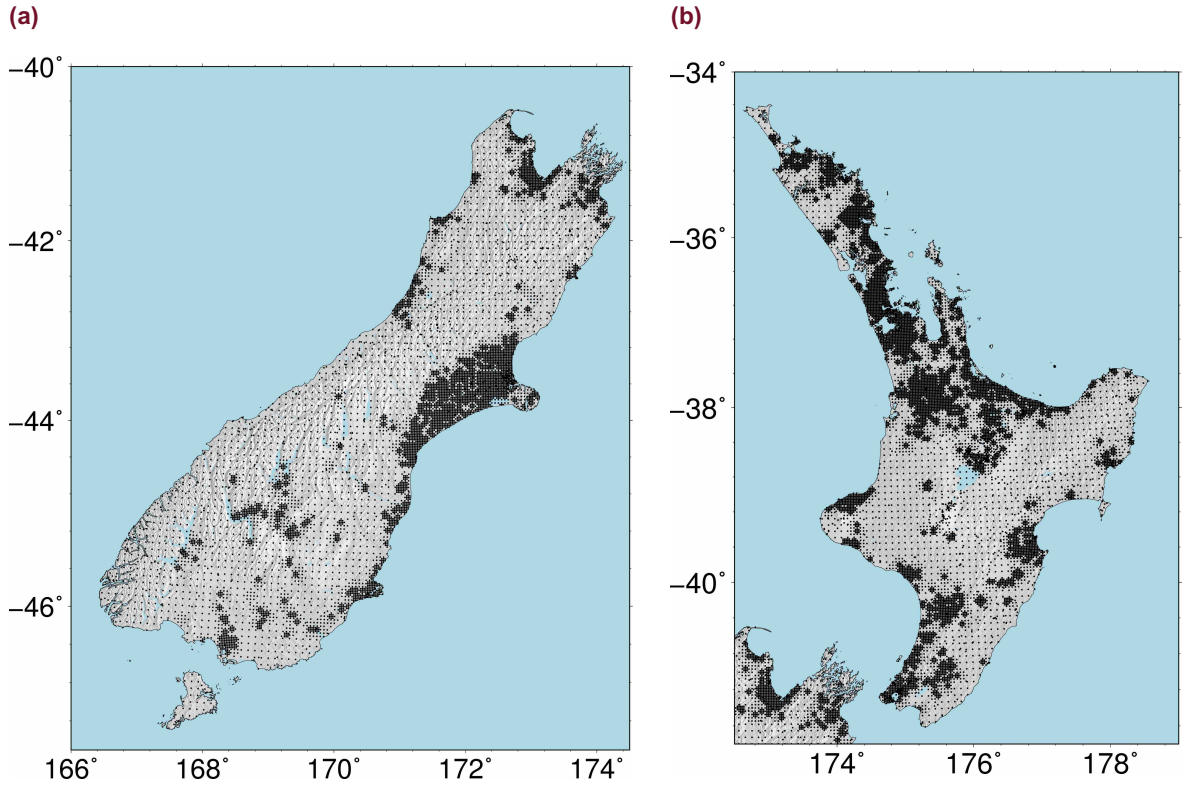

Figure 4. A non-uniform grid generated based on population density and sub-surface soil condition to record simulated ground motions and perform PSHA: (a) South Island; and (b) North Island.

3 PRELIMINARY RESULTS

3.1 Scenario rupture simulations

Figure 5 and Figure 6 present pseudo-spectral acceleration at T=5.0 s vibration period, pSA(5.0 s), of two scenario rupture simulations for HopeConwayOS and AlpineF2K faults. Considering the transition frequency of 0.25, pSA(5.0 s) results are governed by the comprehensive physics-based (i.e. low-frequency) component of hybrid broadband simulations. The results are presented for the geometrical mean of horizontal components for simulated motions, empirical median from Bradley (2013) GMM, and the natural logarithm of the simulated over empirical intensity measure (IM) ratio. These results, among others, illustrate differences in the simulated ground motions in comparison to the empirical estimates (and observed ground motions) as presented extensively elsewhere (e.g., Bradley et al. 2017a, Goulet et al. 2015, Graves et al. 2011, Graves and Pitarka 2010, 2015, Taborda and Bielak 2013). Specifically, simulated ground motions can represent the local basin response in regions with deep sedimentary layers (e.g., Christchurch area on Figure 5a and Figure 6a), directivity effects with respect to the hypocentre location, and rupture-specific spatial variation of ground motions, as opposed to empirical GMMs for which these characteristics are either incorporated via generic/ergodic models (e.g., basin response) or neglected (e.g., forward directivity effects).

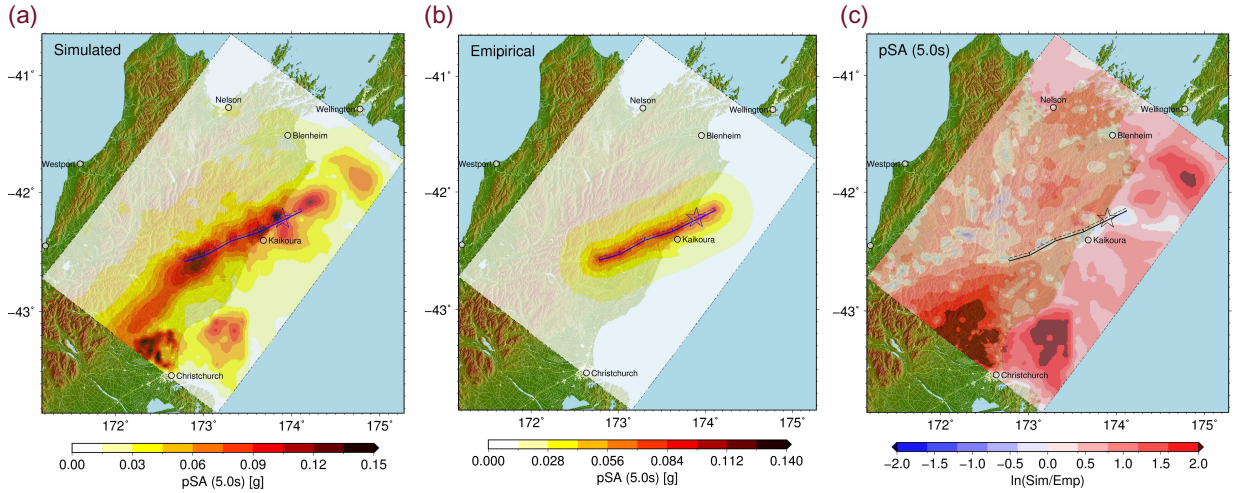

Figure 5. Pseudo spectral acceleration (pSA) at T=5.0 s vibration period from a scenario rupture of HopeConwayOS fault. The results are presented for: (a) geometrical mean of horizontal components for simulated motions; (b) empirical median from Bradley (2013); and (c) natural logarithm of the simulated over empirical IM ratio.

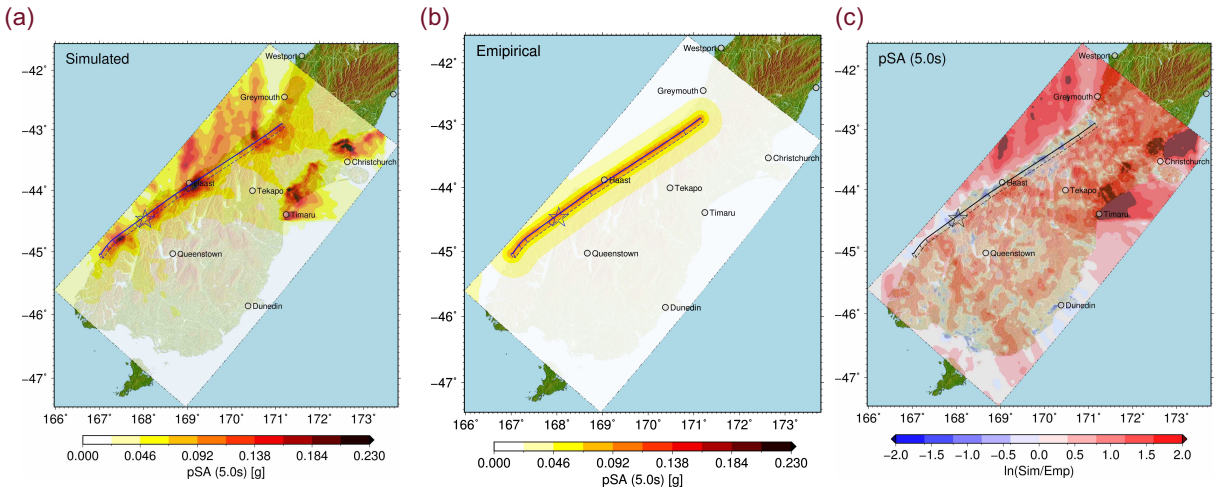

Figure 6. Pseudo spectral acceleration (pSA) at T=5.0 s vibration period from a scenario rupture of AlpineF2K fault. The results are presented for: (a) geometrical mean of horizontal components for simulated motions; (b) empirical median from Bradley (2013); and (c) natural logarithm of the simulated over empirical IM ratio.

3.2 Seismic hazard

PSHA quantifies the annual exceedance frequency (or probability) of a ground motion IM, considering the characteristics of all causative rupture scenarios in the vicinity of the site of interest, using Equation 1:

$$\boldsymbol{\lambda_{IM}(im)} = \sum_{n=1}^{N_{rup}} \boldsymbol{P_{IM|Rup}(im|rup_n)\lambda_{Rup}(rup_n)} \quad (1)$$

where $\lambda_{Rup}(rup_n)$ is the annual frequency of a scenario rupture (rup_n), and $P_{IM|Rup}(im|rup_n)$ is the probability of $IM > im$ given rup_n. In the simulation-based PSHA, $P_{IM|Rup}(im|rup_n)$ is obtained based on the list of IM values from different realizations of rup_n, as opposed to the conventional PSHA where empirical GMMs are utilized. Note that all realizations of hypocentre and slip distribution are considered equally probable here when calculating seismic hazard from simulated ground motions.

Figure 7 illustrates the hazard curves calculated for pSA(5.0 s) at an illustrative site in the Canterbury region [Lat: -43.3759, Lon:172.011], including hazard curves corresponding to three source types: i) distributed seismicity sources for which the hazard curve is calculated using an empirical GMM, i.e., Bradley (2013); ii) finite faults which we have simulated ground motions for, i.e., Type A Faults; and iii) finite faults for which simulations have not presently been conducted and are modelled empirically, i.e., Type B Faults. The total hazard is obtained by adding the hazards from these three sources. The hazard curves for Type A Faults are computed based on both the empirical- and simulation-based models for $P_{IM|Rup}(im|rup_n)$. The Cybershake total hazard curve is calculated by summing the corresponding (Cybershake) Type A fault hazard with the hazard curves from the distributed seismicity sources. The empirical total hazard curve is calculated by summing the empirical Type A, Type B, and distributed seismicity source hazards.

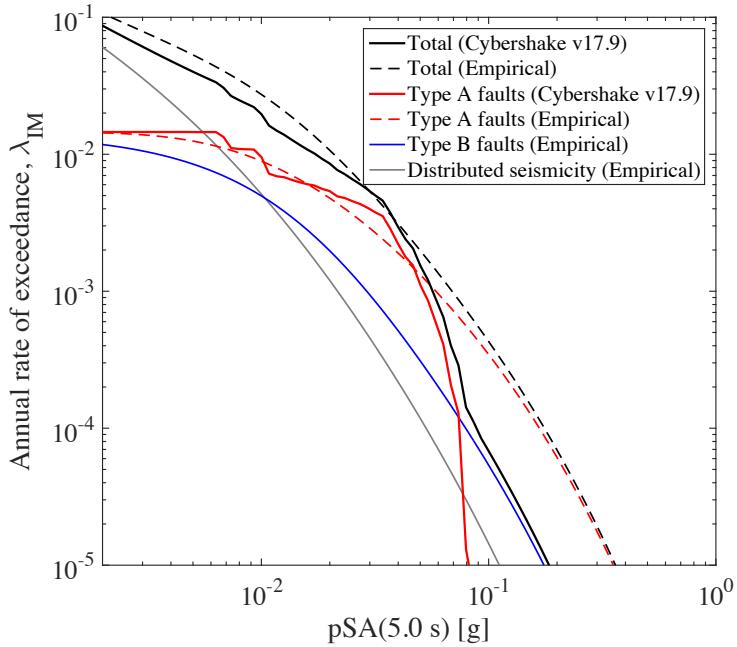

Figure 7. Seismic hazard curves for pSA (5.0 s) (at an illustrative site in the Canterbury region) based on the simulation and empirical approaches.

Figure 7 shows that, due to a small number of realizations for the simulated faults at present, the Cybershake hazard curve for Type A faults (i.e., solid red line) is not as smooth as the empirical counterpart (i.e., dashed red line). Also, for the same reason, simulations do not generally sample IMs at lower exceedance rates. Moreover, the rate of occurrence for faults which have not presently been simulated (i.e., the solid blue line at the lowest IM level) within the 200 km boundary considered for PSHA is high, but this will decrease as the number of simulated faults increases (i.e., the solid blue line will eventually disappear). These issues result in a large difference between the total hazards from the Cybershake v17.9 version and the empirical counterpart. Comparison between the simulation and empirical hazards on a map view (once the ongoing simulations are concluded) can be insightful in determining the differences between these approaches considering the differences in the underlying ground motion modelling principles.

4 DISCUSSION

4.1 Variability in source, path and site effects

In order to partially account for ground motion variability in the 17.9 version of Cybershake NZ, as mentioned before, hypocentres are located at every 20 km along the strike direction and only three slip distributions are considered for each hypocentre realization. In order to obtain a more accurate characterization of the near-fault seismic hazard, a larger number of slip and hypocentre realizations should be considered (Callaghan et al. 2017a, Callaghan et al. 2017b). Variability in parameters such as rupture magnitude, fault dimensions, rupture velocity, rise time, stress drop, and anelastic attenuation should also be progressively considered for future versions of Cybershake NZ.

In order to increase the comprehensive physics-based simulation limit (i.e., transition frequency) of the results, velocity models with a finer discretization (e.g., 0.2 km) will be considered for future versions. In addition, different realizations of the utilized velocity model will be generated in order to investigate the effect of variability in the crustal model (i.e., the path effect) on the obtained ground motions and the resulting seismic hazard curves (which is shown to be significant (e.g., Taborda and Bielak 2014)).

4.2 Epistemic uncertainty

The PSHA formulation presented in Equation 1 takes into account apparent aleatory variability in the occurrence of rupture scenarios and the corresponding ground motions. Note that the hazard curve defined via Equation 1. is conditioned on the adopted GMM (i.e., $P_{IM|Rup}$) and ERF (i.e., λ_{Rup}). Epistemic uncertainty in the PSHA results is conventionally addressed by considering alternative GMMs and ERFs using the logic tree method (Bommer et al. 2005, Kulkarni et al. 1984, Reiter 1991), which results in alternative plausible seismic hazard curves for the site of interest. In this context, simulation-based PSHA can be considered as one of the alternative approaches within the considered logic tree branches, as well as using multiple simulation methods (i.e., simulation-based GMMs) as only one of which was considered here. The weight on the simulation-based PSHA can be assigned based on the validity of simulations in different regions of the country (considering the detailed analyses conducted to examine the validity of simulated ground motions with respect to the observed ground motions).

5 CONCLUSION

This paper presented the computational workflow and preliminary results of the first version of probabilistic seismic hazard analysis (PSHA) based on physics-based ground motion simulations in New Zealand: Cybershake NZ v17.9. The Graves and Pitarka (2010, 2015) method was used to conduct ground motion simulations for the finite faults in Stirling et al. (2012) with a grid spacing of 0.4 km and a transition frequency of 0.25 Hz. Due to the large number of distributed seismicity sources, an empirical ground motion model was used in the hazard calculation for distributed sources. As the available computational resources increase in the future, distributed seismicity sources can be included in the simulation branch of the workflow. Variation in hypocentre location and slip distribution were considered to partially account for the variability in ground motion characteristics. Variability in parameters such as finite fault dimensions, rupture magnitude, rupture velocity, rise time, stress drop, anelastic attenuation, 3D velocity structure, and local site response, among others, will be investigated via sensitivity analyses in order to be progressively considered in future versions. Also, future simulations are envisaged to be conducted on finer grids of 0.2 and 0.1 km in order to utilize simulations for seismic hazard analyses at higher vibration frequencies.

Simulation-based PSHA can directly represent source effects such as directivity in the near-fault region, local characteristics of the crust, and basin responses, as opposed to empirical ground motion models for which these characteristics are either incorporated via generic/ergodic models (e.g., basin response) or neglected (e.g., directivity effects). The simulation-based PSHA presented here is considered as a logic tree branch in New Zealand PSHA in conjunction with branches for alternative rupture characteristics and empirical ground motion models, as well as using multiple simulation-based GMMs.

6 ACKNOWLEDGEMENTS

We gratefully acknowledge the support of New Zealand eScience Infrastructure (NeSI) high-performance computing facility, Royal Society of New Zealand, Natural Hazards Research Platform, and QuakeCoRE: The New Zealand Centre for Earthquake Resilience. This is QuakeCoRE publication 0276.

7 REFERENCES

Bommer, J. J., J. Douglas, F. Scherbaum, F. Cotton, H. Bungum and D. Fäh (2010). "On the selection of ground-motion prediction equations for seismic hazard analysis." Seismological Research Letters **81**(5): 783-793.

Bommer, J. J., F. Scherbaum, H. Bungum, F. Cotton, F. Sabetta and N. A. Abrahamson (2005). "On the use of logic trees for ground-motion prediction equations in seismic-hazard analysis." Bulletin of the Seismological Society of America **95**(2): 377-389.

Bradley, B. A. (2013). "A New Zealand-Specific Pseudospectral Acceleration Ground-Motion Prediction Equation for Active Shallow Crustal Earthquakes Based on Foreign Models." Bulletin of the Seismological Society of America **103**(3): 1801-1822.

Bradley, B. A., S. E. Bae, V. Polak, R. L. Lee, E. M. Thomson and K. Tarbali (2017a). "Ground motion simulations of great earthquakes on the Alpine Fault: effect of hypocentre location and comparison with empirical modelling." New Zealand Journal of Geology and Geophysics: 1-11.

Bradley, B. A., H. N. Razafindrakoto and V. Polak (2017b). "Ground-Motion Observations from the 14 November 2016 M w 7.8 Kaikoura, New Zealand, Earthquake and Insights from Broadband Simulations." Seismological Research Letters **88**(3): 740-756.

Callaghan, S., R. W. Graves, K. B. Olsen, Y. Cui, K. R. Milner, C. A. Goulet, P. J. Maechling and T. H. Jordan (2017a). 10 years of CyberShake: Where are we now and where are we going with physics-based PSHA? 2017 Southern California Earthquake Center Annual Meeting.

Callaghan, S., P. J. Maechling, C. A. Goulet, K. R. Milner, R. W. Graves, K. B. Olsen and T. H. Jordan (2017b). CyberShake: bringing physics-based PSHA to central California. Poster Presentation at 2017 SCEC Annual Meeting. . 2017 Southern California Earthquake Center Annual Meeting, Poster #303.

Campbell, K. W. and Y. Bozorgnia (2014). "NGA-West2 ground motion model for the average horizontal components of PGA, PGV, and 5% damped linear acceleration response spectra." Earthquake Spectra **30**(3): 1087-1115.

Eberhart-Phillips, D., M. Reyners, S. Bannister, M. Chadwick and S. Ellis (2010). "Establishing a versatile 3-D seismic velocity model for New Zealand." Seismological Research Letters **81**(6): 992-1000.

Goulet, C. A., N. A. Abrahamson, P. G. Somerville and K. E. Wooddell (2015). "The SCEC broadband platform validation exercise: Methodology for code validation in the context of seismic-hazard analyses." Seismological Research Letters **86**(1): 17-26.

Graves, R., T. H. Jordan, S. Callaghan, E. Deelman, E. Field, G. Juve, C. Kesselman, P. Maechling, G. Mehta and K. Milner (2011). "CyberShake: A physics-based seismic hazard model for southern California." Pure and Applied Geophysics **168**(3-4): 367-381.

Graves, R. and A. Pitarka (2010). "Broadband ground-motion simulation using a hybrid approach." Bulletin of the Seismological Society of America **100**(5A): 2095-2123.

Graves, R. and A. Pitarka (2015). "Refinements to the Graves and Pitarka (2010) broadband ground-motion simulation method." Seismological Research Letters **86**(1): 75-80.

King, G. C. and S. G. Wesnousky (2007). "Scaling of fault parameters for continental strike-slip earthquakes." Bulletin of the Seismological Society of America **97**(6): 1833-1840.

Kulkarni, R., R. Youngs and K. Coppersmith (1984). Assessment of confidence intervals for results of seismic hazard analysis. Proceedings of the Eighth World Conference on Earthquake Engineering.

Lee, R. L., B. A. Bradley, F. C. Ghisetti and E. M. Thomson (2017). "Development of a 3D Velocity Model of the Canterbury, New Zealand, Region for Broadband Ground-Motion Simulation." Bulletin of the Seismological Society of America **107**(5): 2131-2150.

Leonard, M. (2010). "Earthquake fault scaling: Self-consistent relating of rupture length, width, average displacement, and moment release." Bulletin of the Seismological Society of America **100**(5A): 1971-1988.

Mai, P. M., P. Spudich and J. Boatwright (2005). "Hypocenter locations in finite-source rupture models." Bulletin of the Seismological Society of America **95**(3): 965-980.

Reiter, L. (1991). Earthquake hazard analysis: issues and insights, Columbia University Press.

Roten, D., K. Olsen, S. Day and Y. Cui (2017). "Quantification of fault-zone plasticity effects with spontaneous rupture simulations." Pure and Applied Geophysics **174**(9): 3369-3391.

Stirling, M., G. McVerry, M. Gerstenberger, N. Litchfield, R. Van Dissen, K. Berryman, P. Barnes, L. Wallace, P. Villamor and R. Langridge (2012). "National seismic hazard model for New Zealand: 2010 update." Bulletin of the Seismological Society of America **102**(4): 1514-1542.

Strasser, F. O., N. A. Abrahamson and J. J. Bommer (2009). "Sigma: Issues, insights, and challenges." Seismological Research Letters **80**(1): 40-56.

Taborda, R., S. Azizzadeh-Roodpish, N. Khoshnevis and K. Cheng (2016). "Evaluation of the southern California seismic velocity models through simulation of recorded events." Geophysical Journal International **205**(3): 1342-1364.

Taborda, R. and J. Bielak (2013). "Ground-motion simulation and validation of the 2008 Chino Hills, California, earthquake." Bulletin of the Seismological Society of America **103**(1): 131-156.

Taborda, R. and J. Bielak (2014). "Ground-motion simulation and validation of the 2008 Chino Hills, California, earthquake using different velocity models." Bulletin of the Seismological Society of America.

Taborda, R., J. Bielak and D. Restrepo (2012). "Earthquake ground-motion simulation including nonlinear soil effects under idealized conditions with application to two case studies." Seismological Research Letters **83**(6): 1047-1060.